

Towards the Industrial Solar Carbothermal Production of Zinc

Michael Epstein

Solar Research Unit,
The Weizmann Institute of Science,
IL-76100 Rehovot, Israel

Gabriel Olalde

PROMES-CNRS,
Odeillo,
F-66125 Font-Romeu, France

Sven Santén

ScanArc Plasma Technologies AB,
S-81321 Hofors, Sweden

Aldo Steinfeld

Department of Mechanical and Process Engineering,
ETH Zurich,
CH-8092 Zurich, Switzerland

Christian Wieckert¹

Solar Technology Laboratory,
Paul Scherrer Institute,
CH-5232 Villigen, Switzerland
e-mail: christian.wieckert@psi.ch

Based on the experimental results of a 300 kW solar chemical pilot plant for the production of zinc by carbothermal reduction of ZnO, we performed a conceptual design of a 5 MW demonstration plant and of a 30 MW commercial plant. Zinc can be used as a fuel for zinc-air batteries and fuel cells, or it can be reacted with water to form high-purity hydrogen. In either case, the chemical product is ZnO, which in turn is solar recycled to zinc. The proposed thermochemical process provides an energy efficient route for the conversion, storage, and transportation of solar energy in the form of solar fuels. [DOI: 10.1115/1.2807214]

Keywords: solar, energy, fuel, hydrogen, zinc, carbothermal, reduction, concentrated

Introduction

Solar-made zinc offers the possibility of storing and transporting solar energy in chemical form [1]. It is a compact solid fuel that can be used in Zn/air fuel cells and batteries. Zinc can also react with water in a slightly exothermic reaction to form high-purity hydrogen [2–4]. In either case, the chemical product from these power generation processes is ZnO, which in turn is solar reduced to Zn. This two-step cyclic process can be described as:



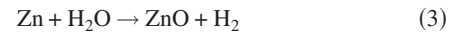
electricity generation step,

¹Corresponding author.

Contributed by the Solar Energy Engineering Division of ASME for publication in the JOURNAL OF SOLAR ENERGY ENGINEERING. Manuscript received February 23, 2007; final manuscript received June 9, 2007; published online January 7, 2008. Review conducted by Manuel Romero Alvarez.



hydrogen generation step,



The CO product of the solar step may be used as a fuel or can be water-gas shifted to H₂. The solar carbothermal reduction of ZnO has been experimentally demonstrated in solar furnaces using carbon [5–8] and methane [9] as reducing agents. Equation (1) proceeds endothermally ($\Delta H_{1500 \text{ K}}^\circ = 350 \text{ kJ/mol}$) at above 1200 K. Industrial beech wood charcoal was selected as the reducing agent because of the relatively fast reaction rate at 1300 K as compared to other carbon sources [8]. Using petcoke would require about 200 K higher operational temperature for obtaining the same specific reaction rate as that obtained using charcoal [8]. From the standpoint of CO₂ avoidance, the solar-driven carbothermal production of Zn results in a five-fold reduction of the CO₂ emissions vis-à-vis the conventional fossil-fuel-driven electrolytic or imperial smelting processes (relevant, if commodity zinc is produced) and in a two-fold reduction for the cyclic processes to electricity or hydrogen. Obviously, if biomass is used as a reducing agent, the two-step process has zero-net CO₂ emissions. The solar contribution accounts for more than 45% of the initial calorific value of the reactants.

Recently, within the framework of the EU-SOLZINC project, a 300 kW solar chemical pilot plant for the carbothermal production of zinc was built and successfully operated in a beam-down solar tower facility [10]. The solar chemical reactor consisted of two cavities, of which the upper one functioned as the solar absorber and the lower one as the reaction chamber containing a ZnO/C packed bed. The reactor was operated in a one-batch-per-day mode in the temperature range 1300–1500 K and yielded up to 50 kg/h of 95%-purity Zn. The measured solar-to-fuel energy conversion efficiency, defined as the ratio of the reaction enthalpy change to the solar power input, was up to 30%. The quenching system at the exit of the solar reactor used recycled cold product gas (mainly CO) to dilute the hot products emerging out from the reactor and produced zinc dust with typical particle size of a few microns. Based on the operational results and the hardware experience obtained in this previous project, a conceptual design of a 5 MW demo plant and a 30 MW commercial plant is outlined in this paper.

Conceptual Optical Design of a 5 MW Demonstration Plant and a 30 MW Commercial Plant

Figure 1 shows schematically the layout for a beam-down solar concentrating system of Cassegrain optical configuration [11]. The main components are the heliostat field (HF), the tower reflector (TR), and the array of compound parabolic concentrators (CPCs). Their optical design parameters were determined to provide about 5 MW and 30 MW of concentrated solar radiation at the aperture of the receiver-reactor at the design point (equinox, noon time, Rehovot) [12]. These parameters, along with the energetic aspects of the solar chemical plant, are summarized in Table 1.

The HF's specifications are based on the existing solar tower facility of the Weizmann Institute of Science. Each heliostat consists of 20 facets with a total surface of $7.72 \times 7.85 \text{ m}^2$, providing 89.25% net reflective area of average reflectivity 0.9. The tracking error in each axis is 0.4 mrad and the surface error is 1.1 mrad. All heliostats are canted to the same aim point: the TR's upper focus. The TR is made of a large number of flat plane mirrors, of reflectivity 0.95, which approximate the geometrical shape of the upper sheet of a hyperboloid of revolution. Its position, defined by f as the height of the TR relative to distance to the upper focus, determines its size and the radiative flux incident on the mirrors. There is an upper limit to the radiative flux allowed on the TR as current practice is to passively cool the reflector by natural convection. This upper limit, dictated by the materials of construction, is 35 kW/m^2 , which can develop into temperatures up to

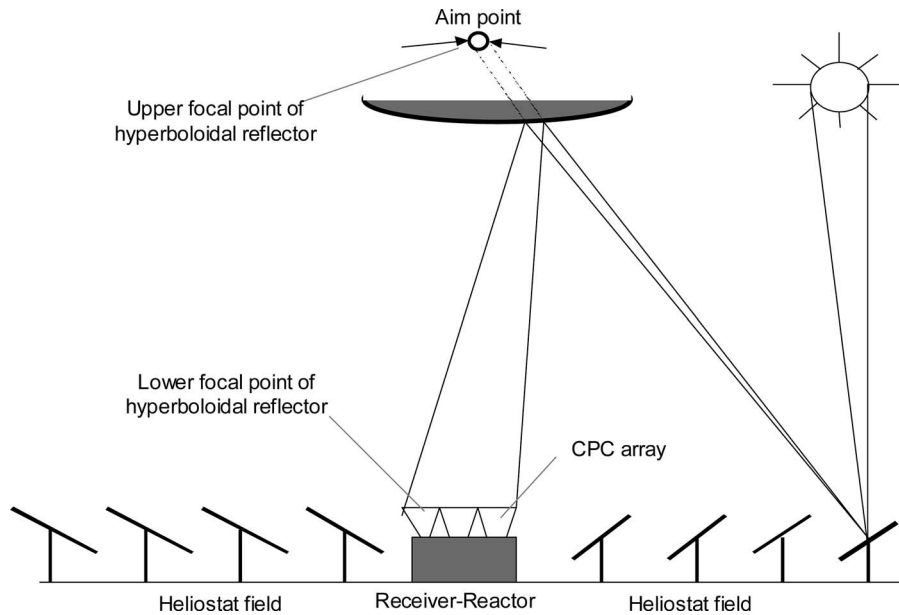


Fig. 1 Optical path of the beam-down solar tower concentrating system (Cassegrain optical configuration), featuring a heliostat field, a tower hyperbolic reflector, and an array of CPCs

130–140°C at the back of the reflecting mirrors. The terminal concentrator comprises an array of seven identical CPC units of hexagonal cross section. They are arranged with one in the center and six peripherals, as shown in Fig. 2. This arrangement was found to be more practical from the construction point of view and led to a superior distribution of the solar radiation input inside the reactor as compared to the single CPC design. The CPC's surface has a 95% reflectivity and is water cooled.

The HF's layouts of the 5 MW and the 30 MW plants are depicted in Fig. 3. A north field is conceived for the 5 MW plant. It

comprises 186 heliostats—corresponding to a reflective area of 10,063 m²—with a 70 m height aim point, resulting in an average shadowing and blocking at design points of 0.65% and 2.5%, respectively. A surrounding field is conceived for the 30 MW plant. It comprises 1144 heliostats—corresponding to a reflective area of 61,876 m²—with a 70 m height aim point. Two CPC's exit diameters of 1.5 m and 1.6 m are analyzed to illustrate the effect of the window size for the reactor aperture on the geometrical parameters of the CPC and its energy delivery. The surface

Table 1 Optical design parameters of 5 MW and 30 MW solar chemical plants

	5 MW	30 MW	
Production capacity	1.7 ton Zn/h	10 ton Zn/h	
Height of HF aim point (upper focus of the TR) (m)	70	140	
Height of the TR (m)	59	118.2	
f ratio=height of TR/height of HF aim point	0.825	0.83	
HF reflective area (m ²)	10,063	61,876	
No. of heliostats	186	1,144	
HF land area (m ²)	28,750	176,800	
TR reflective area (m ²)	285	2,034	
Percent of HF area (%)	2.8	3.3	
Solar radiation intercepted by the TR (kW)	6,703	37,875	
Spillage around TR (kW)	40	372	
Percent of total power (%)	0.6	0.97	
Maximum flux on TR (kW/m ²)	37.6	28.1	
Power arriving at the CPC entrance plane (kW)	6,285	35,162	
Spillage around the CPC entrance aperture (kW)	489	3,016	2,152
Spillage ratio of power arriving at CPC entrance (%)	7.8	8.6	6.1
Power enters the CPC (kW)	5,796	32,146	33,010
Power losses in CPC due to rejection/absorption (kW)	374	1,192	1,398
Power exit from CPC (kW)	5,422	30,134	30,966
Exit diameter of single CPC unit (m)	0.8	1.5	1.6
CPC exit area (m ²)	0.5	1.767	2.0
Average exit concentration	1,550	2,436	2,212
CPC total reflective area (m ²)	409	1,092	1,246
Percent of HF area (%)	4.06	1.76	2.01
CPC acceptance angle (°)	13.5	15	15
Height of CPC unit (m)	8.8	13.6	14.5

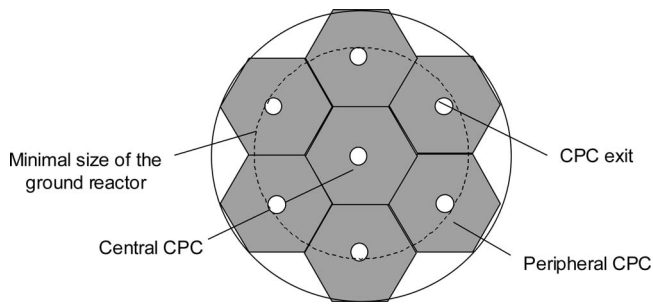


Fig. 2 Arrangement of the array of seven hexagonal CPC units

areas of the TR and the CPC are also indicated as a fraction of the heliostats reflective surface, as these are the parameters needed for further economical optimization, as well as for minimization of radiation spillage around the TR and the entrance perimeter of the CPC units.

Two approaches have been examined for the scaleup of the one-batch-per-day solar reactor. In the first one, all the exits of the seven CPCs match seven openings of the ceiling of a single reac-

tor vessel. In this case, the reactor inner diameters are 8 m and 20 m for the 5 MW and the 30 MW plant, respectively. The average flux on the radiating plate separating the upper and the lower cavity of the reactor is in the range 100–120 kW/m². The net flux incident at the surface of the reactants and absorbed by the endothermic process is about 60 kW/m². The carbothermal reduction is assumed to proceed at 1150–1200°C and at a rate of about 35 kg Zn/h and m², as obtained experimentally in the 300 kW pilot plant [10]. In the second approach, seven solar reactor modules are positioned under each CPC. For the 5 MW plant, the central module has a 3.5 m inner diameter and the peripheral ones have 2 m inner diameter. In this case, the average flux on the radiating plate is 200 kW/m². The single reactor approach requiring only a single Zn quench offgas system was selected for further consideration. Figure 4 shows a sketch of the 5 MW solar reactor design [13].

Table 2 lists the geometrical and energetic design parameters for the 5 MW and 30 MW solar reactors. The predicted solar-to-fuel energy conversion efficiencies, defined as the net solar energy absorbed in the chemical reaction (e.g., enthalpy change) divided by the amount of solar radiation emerging out of the CPC and entering the solar reactor, are 57% and 64% for the 5 MW and 30 MW solar reactor, respectively, as estimated based on energy

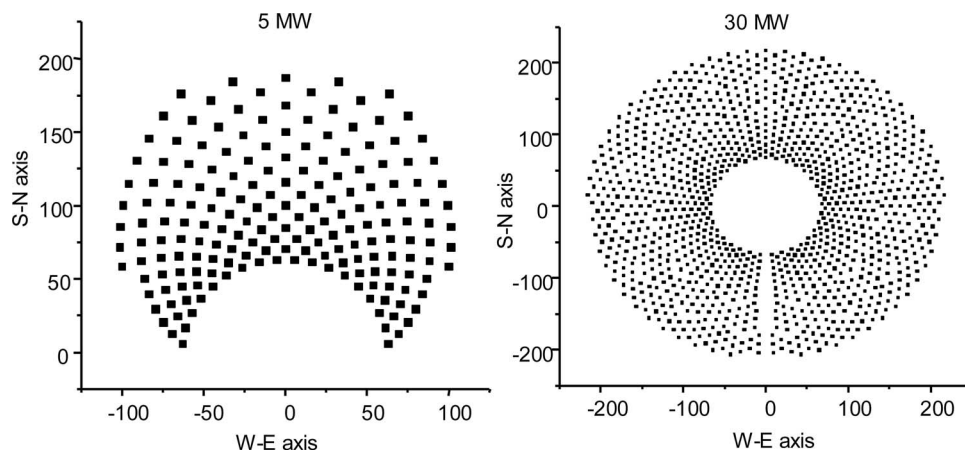


Fig. 3 Heliostat field layout of a 5 MW north-field solar plant with 186 heliostats (10,063 m²) for a 70 m height aim point and a 30 MW surrounding-field solar plant with 1144 heliostats (61,876 m²) for a 140 m height aim point

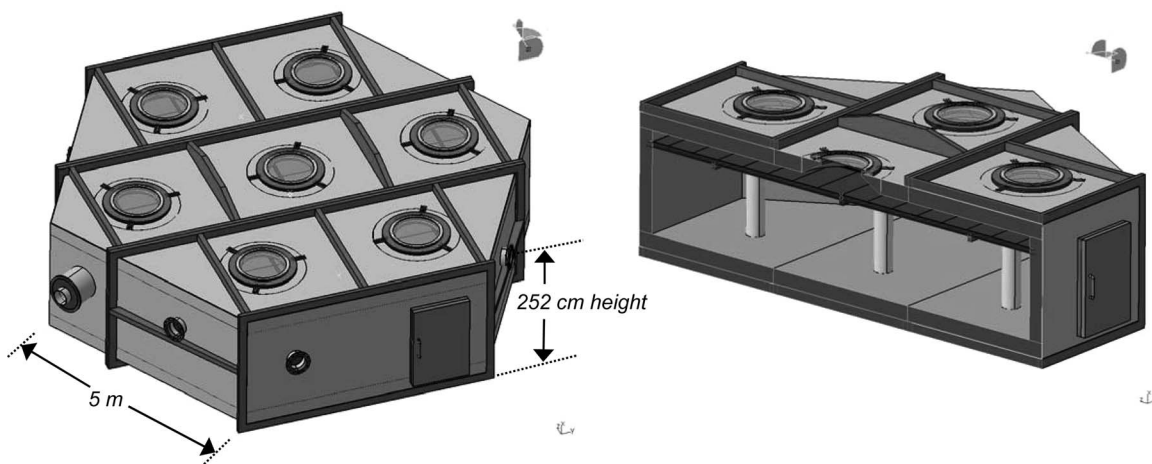


Fig. 4 Conceptual design of a 5 MW solar reactor featuring seven apertures matching the exits of the CPCs, one common upper cavity serving as the absorber of concentrated solar radiation, and one common lower cavity serving as the reaction chamber

Table 2 Design parameters for the 5 MW and 30 MW solar chemical reactors

Plant size	5 MW	30 MW
Carbon to ZnO molar ratio	0.8	0.8
Reaction rate (kmol/m ² /h)	0.54	0.54
Bed shrinking rate (m/h)	0.0775	0.0775
Reactor diameter (m)	8.0	20
Reacting bed surface area (m ²)	50.3	314.2
Total aperture area of seven openings (m ²)	3.5	14
Effective aperture diameter (m)	2.12	4.24
Height of lower cavity (m)	1.5	1.5
Height of upper cavity (m)	0.3	0.3
Diameter of upper cavity (m)	8.0	20
Average thermal losses through walls (kW/m ²)	5.0	5.0
Total thermal losses through walls (kW)	711	3,636
Total losses via reradiation (kW)	1305	5,555
Other thermal losses (kW)	253	1,399
Reaction rate (kg Zn/h)	1780	11,100
Total input energy into the reaction and sensible heat (kW)	2990	18,685
Total solar power input (kW)	5315	29,387
Total energy conversion efficiency of the reactor (%)	57	64

balances on the 300 kW pilot test [10]. An offgas/quench system for the production of Zn dust similar to the one tested in the 300 kW pilot plant is envisioned, but the production of other forms of Zn (e.g., powder or bulk Zn) may be adapted as well [14].

4 Summary and Conclusions

We have conceptually designed a beam-down solar tower system coupled with an array of CPCs for providing concentrated solar energy at megawatt-scale power level to a one-batch-per-day solar reactor for the carbothermal production of Zn. The predicted solar-to-fuel energy conversion efficiency of the 5 MW solar chemical reactor is 57% (based on the solar power input into the reactor) using a HF of about 10,000 m² on a 200 × 200 m² land area and producing 1.7 ton Zn/h. The predicted energy conversion efficiency of the 30 MW solar chemical reactor is 64%, using a HF of about 62,000 m² on a 400 × 400 m² land area and producing 11 ton Zn/h. The main sources of energy losses are radiative spillage around the CPCs, reradiation from the solar reactor, and heat conduction through the reactor walls. The produced zinc al-

lows for solar energy storage and transport, and its use for electricity generation via Zn-air fuel cells or for H₂ generation via steam hydrolysis.

Acknowledgment

Funding by the EU (Project SOLZINC, Contract No. ENK6-CT2001-00512) and by the SER-Swiss State Secretariat for Education and Research is gratefully acknowledged.

References

- [1] Steinfeld, A., Kuhn, P., Reller, A., Palumbo, R., Murray, J., and Tamaura, Y., 1998, "Solar-Processed Metals as Clean Energy Carriers and Water-Splitters," *Int. J. Hydrogen Energy*, **23**(9), pp. 767–74.
- [2] Berman, A., and Epstein, M., 2000, "The Kinetics of Hydrogen in the Oxidation of Liquid Zinc With Water Vapor," *Int. J. Hydrogen Energy*, **25**, pp. 957–967.
- [3] Wegner, K., Ly, H., Weiss, R., Pratsinis, S., and Steinfeld, A., 2006, "In-Situ Formation and Hydrolysis of Zn Nanoparticles for H₂ Production by the 2-Step ZnO/Zn Water-Splitting Thermochemical Cycle," *Int. J. Hydrogen Energy*, **31**, pp. 55–61.
- [4] Ernst, F., Tricoli, A., Steinfeld, A., Pratsinis, S., and Steinfeld, A., 2006, "Co-Synthesis of H₂ and ZnO by In-Situ Aerosol Formation and Hydrolysis," *AIChE J.*, **52**, pp. 3297–3303.
- [5] Murray, J., Steinfeld, A., and Fletcher, E., 1995, "Metals, Nitrides, and Carbides Via Solar Carbothermal Reduction of Metals Oxides," *Energy*, **20**, pp. 695–704.
- [6] Adinberg, R., and Epstein, M., 2004, "Experimental Study of Solar Reactors for Carboreduction of Zinc Oxide," *Energy*, **29**, pp. 757–769.
- [7] Osinga, T., Frommherz, U., Steinfeld, A., and Wieckert, C., 2004, "Experimental Investigation of the Solar Carbothermal Reduction of ZnO Using a Two-Cavity Solar Reactor," *ASME J. Sol. Energy Eng.*, **126**, pp. 633–637.
- [8] Kräupl, S., Frommherz, U., and Wieckert, C., 2006, "Solar Carbothermal Reduction of ZnO in a Two Cavity Reactor: Laboratory Experiments for a Reactor Scale-Up," *ASME J. Sol. Energy Eng.*, **128**, pp. 8–15.
- [9] Kräupl, S., and Steinfeld, A., 2001, "Experimental Investigation of a Vortex-Flow Solar Chemical Reactor for the Combined ZnO-Reduction and CH₄-Reforming," *ASME J. Sol. Energy Eng.*, **123**, pp. 237–243.
- [10] Wieckert, C., Guillot, E., Epstein, M., Olalde, G., Santén, S., Frommherz, U., Kräupl, S., Osinga, T., and Steinfeld, A., 2007, "A 300 kW Solar Chemical Pilot Plant for the Carbothermal Production of Zinc," *ASME J. Sol. Energy Eng.*, **129**, pp. 190–196.
- [11] Segal, A., and Epstein, M., 1999, "Comparative Performances of Tower-Top and Tower-Reflector Central Solar Receivers," *Sol. Energy*, **65**, pp. 206–226.
- [12] Segal, A., and Epstein, M., 1996, "A Model for Optimization of a Heliostat Field Layout," in *Proceedings of the Eighth International Symposium on Solar Thermal Concentrating Technologies*, Cologne, Germany, Oct. 6–11, Becker, M., and Böhmen, M., eds., C.F. Müller Verlag, Heidelberg, pp. 989–998.
- [13] Wieckert, C., Epstein, M., Olalde, G., Santén, S., and Steinfeld, A., 2006, "Pilot Scale Solar Carbothermal Reduction of ZnO to Zn," in *Proceedings Sohn International Symposium on Advanced Processing of Metals and Materials*, Aug. 27–31, Kongoli, F., and Reddy, R. G., eds., The Minerals, Metals and Materials Society, pp. 221–236.
- [14] Epstein, M., Olalde, G., Santén, S., Steinfeld, A., and Wieckert, C., 2006, "Solar Thermochemical Production of Hydrogen—The Carbothermal ZnO/Zn Cyclic Process," *Proceedings World Hydrogen Energy Conference*, Lyon, France, Jun. 13–16.